Elastic Scattering and Reaction Mechanisms of the Halo Nucleus 11Be around the Coulomb Barrier

Di Pietro, A.; Randisi, G.; Scuderi, V.; Acosta, L.; Amorini, F.; Borge, M. J. G.; Figuera, P.; Fisichella, M.; Fraile, L. M.; Gomez-Camacho, J.; ...

Source / Izvornik: **Physical Review Letters, 2010, 105**

Journal article, Published version
Rad u časopisu, Objavljena verzija rada (izdavačev PDF)

https://doi.org/10.1103/PhysRevLett.105.022701

Permanent link / Trajna poveznica: https://urn.nsk.hr/urn:nbn:hr:217:089918

Elastic Scattering and Reaction Mechanisms of the Halo Nucleus ^{11}Be around the Coulomb Barrier

A. Di Pietro,[1] G. Randisi,[1,2,*] V. Scuderi,[1,2] L. Acosta,[3] F. Amorini,[1,2] M. J. G. Borge,[4] P. Figuera,[1] M. Fisichella,[1,2] L. M. Fraile,[5,†] J. Gomez-Camacho,[6] H. Jeppesen,[5,‡] M. Lattuada,[1,2] I. Martel,[3] M. Milin,[7] A. Musumarra,[1,8] M. Papa,[1] M. G. Pellegriti,[1,2] F. Perez-Bernal,[3] R. Raabe,[9] F. Rizzo,[1,2] D. Santonocito,[1] G. Scalia,[1,2] O. Tengblad,[4] D. Torresi,[1,2] A. Maira Vidal,[4] D. Voulot,[5] F. Wenander,[5] and M. Zadro[10]

[1]*INFN–Laboratori Nazionali del Sud and Sezione di Catania, Catania, Italy*
[2]*Dipartimento di Fisica ed Astronomia, Universitá di Catania, Catania, Italy*
[3]*Departamento de Fisica Aplicada, Universidad de Huelva, Huelva, Spain*
[4]*Instituto de Estructura de la Materia CSIC, Madrid, Spain*
[5]*ISOLDE, CERN, CH-1211 Geneva 23, Switzerland*
[6]*Departamento de Fisica Atomica Molecular Nuclear, Universidad de Sevilla and Centro Nacional de Aceleradores, Sevilla, Spain*
[7]*Department of Physics, Faculty of Science, University of Zagreb, Zagreb, Croatia*
[8]*Dipartimento di Metodologie Fisiche e Chimiche per l'Ingegneria, Universitá di Catania, Catania, Italy*
[9]*Instituut voor Kern-en Stralingsfysica, Katholieke Universiteit, Leuven, Belgium*
[10]*Division of Experimental Physics, Ruđer Bošković Institute, Zagreb, Croatia*

(Received 7 March 2010; published 6 July 2010)

Collisions induced by ^{9,10,11}Be on a ^{64}Zn target at the same c.m. energy were studied. For the first time, strong effects of the ^{11}Be halo structure on elastic-scattering and reaction mechanisms at energies near the Coulomb barrier are evidenced experimentally. The elastic-scattering cross section of the ^{11}Be halo nucleus shows unusual behavior in the Coulomb-nuclear interference peak angular region. The extracted total-reaction cross section for the ^{11}Be collision is more than double the ones measured in the collisions induced by ^{9,10}Be. It is shown that such a strong enhancement of the total-reaction cross section with ^{11}Be is due to transfer and breakup processes.

DOI: 10.1103/PhysRevLett.105.022701 PACS numbers: 25.60.Bx, 25.70.Bc

A hundred years after Rutherford's α scattering experiment [1], heavy-ion-elastic-scattering angular distributions (AD) are usually plotted as a ratio of the Rutherford cross section (i.e., pure Coulomb scattering). Such representation usually shows a decrease of the elastic cross section with the angle due to absorption at small impact parameters by nonelastic processes, and an oscillatory behavior. The latter, using the language of optics, is described in terms of refraction by nonabsorbing lenses (Coulomb rainbow model) or diffraction by sharp-edged, nonrefracting apertures (Fraunhofer or Fresnel diffraction model). However, the refraction or diffraction descriptions are oversimplifications of the realistic process; rather, the nucleus behaves as a ''cloudy crystal ball.'' The elastic-scattering AD may show a peak resulting from the interference between the Coulomb and nuclear amplitudes (Coulomb-nuclear interference peak) [2], which, in analogy with the Coulomb rainbow model, is sometimes called the rainbow peak. Since elastic scattering is a peripheral process, it does not give information on the interior region of nuclei. It probes the tail of the wave function, and hence one can learn about surface properties, such as size of nuclei and surface diffuseness. Therefore, elastic scattering is an ideal tool to study peculiar nuclear structures as, for example, the nuclear halo. Such structure originates when very weakly bound nucleon(s) can tunnel into the classically forbidden region, giving rise to a diffuse tail surrounding a well-bound core. The behavior of the system in nuclear reactions is mostly determined by the tail of the wave function [3]. The reaction mechanisms may also be affected by the weak binding: at energies around the Coulomb barrier, couplings between the entrance channel and the continuum [4–8], as well as to the various reaction channels [9–12], are expected to be very important. Direct reactions, such as breakup or transfer, may be favored owing to the low binding energy, the extended tail of halo nuclei, and the large Q values for selected transfer channels.

Almost all elastic-scattering and reaction mechanism studies around the barrier with halo nuclei have been performed with the $2n$ halo nucleus ^{6}He. All authors agree that, due to the ^{6}He structure, one has an enhancement of the total-reaction (TR) cross section due to strong transfer and breakup channels which may saturate almost completely the TR cross section at and below the barrier (e.g., [10,13–15]). To our knowledge, only two attempts to measure elastic-scattering and reaction mechanisms around the barrier with n-halo nuclei different from ^{6}He are reported in literature. In [16,17] ^{11}Be + ^{209}Bi, the quasielastic cross section, which included inelastic excitations up to 2.6 MeV, was measured using a fragmentation beam degraded in energy. At energies exceeding 10% of

the barrier, the extracted TR cross section was found to be similar to the one of ^{9}Be + ^{209}Bi. In [18] ^{11}Be + ^{120}Sn, quasi-elastic-scattering [the ^{11}Be($\frac{1}{2}^{-}$) inelastic excitation was included] AD was measured, but in a very limited angular range.

This Letter reports, for the first time, clear experimental evidence of strong effects of the ^{11}Be halo structure on elastic-scattering and reaction mechanisms in collisions close to the Coulomb barrier. We measured high quality elastic-scattering AD of ^{9,10,11}Be on a ^{64}Zn target, in a wide angular range and with small angular step, at $E_{\mathrm{c.m.}} \approx$ 24.5 MeV, corresponding to about 1.4 the Coulomb barrier. Moreover, in the case of the ^{11}Be halo nucleus, the breakup or transfer AD was extracted. The three beryllium isotopes have different structures, namely, ^{9}Be is a Borromean weakly bound nucleus ($S_n = 1.67$ MeV), with a well-developed α-α-n cluster structure (see, e.g., [19]). With an additional nucleon and due to pairing, ^{10}Be in its ground state is equally deformed but much more bound ($S_n = 6.81$ MeV) than ^{9}Be. Finally, ^{11}Be is a one neutron halo nucleus whose core is ^{10}Be and its binding energy is only $S_n = 503$ keV [20]. By comparing the elastic-scattering AD for these three systems, the separate effect of the weak binding and halo structure can be investigated.

The data with the radioactive beams were obtained, in the same experiment, using the new postaccelerated ^{10,11}Be beams of REX-ISOLDE at CERN. The detection system used consisted of an array of Si-detector telescopes each formed by a 40 μm, 50 $\times$ 50 mm^2, ΔE DSSSD detector (16 $\times$ 16 pixels) and a 1500 μm single pad E detector. The detectors were placed very close to the target in order to have a large angular ($10^\circ \leq \theta \leq 150^\circ$) and solid angle coverage. Because of the high granularity, the AD could be obtained with a 1° step. The beam energy resolution was insufficient to separate ^{11}Be elastic from inelastic scattering of the ^{11}Be 1st excited state at $E_x = 320$ keV, but as we will see in the following, the inelastic channel contributes very little to the measured AD. A 550 and 1000 μg/cm^2 ^{64}Zn target was used with ^{10}Be and ^{11}Be beams, respectively. The target was tilted at 45° to facilitate the measurement in the angular region around 90°. The average beam intensity was 10^6 and 10^4 pps for ^{10}Be and ^{11}Be, respectively. Because of the very compact geometry of the detection system, small variations of the beam position onto the target resulted in a non-negligible variation of the detector angles. Therefore, particular care was taken in the off-line analysis, to reconstruct the correct detector angles. This was done by looking at the small angle Rutherford scattering in the two front detectors placed symmetrically with respect to the beam axis. In order to check the adopted procedure, ^{12}C, ^{10}Be + ^{197}Au elastic-scattering at energies $E_{\mathrm{c.m.}} = 25.7$ and 27.9 MeV, respectively, was also measured and the expected Rutherford cross sections were obtained. The experiment with the stable ^{9}Be beam was performed at Laboratori Nazionali del Sud (LNS) in Catania. The ^{9}Be beam was delivered by the 14 MV SMP Tandem of LNS and was impinging on a 550 μg/cm^2 ^{64}Zn target. Five Si-detector telescopes (10 μm ΔE and 200 μm E detectors), placed on a rotating arm, allowed the measurement of the elastic-scattering AD up to 110°.

In Fig. 1 the AD for the scattering of ^{9,10,11}Be + ^{64}Zn are shown in linear scale. As one can see, in spite of the very different binding energies of ^{9}Be and ^{10}Be, their elastic-scattering AD are similar. ^{11}Be scattering shows a very different pattern; the main feature that one can observe in Fig. 1 is a dramatic reduction of the elastic cross section at forward angles. A similar reduction of the elastic cross section is observed in collisions involving deformed nuclei [21] where it arises from coupling with the strong Coulomb excitation of the 2^+ state in the target. In [4] the effect of coupling with a large Coulomb dipole excitation due to the presence of the continuum low-lying $E1$ strength is investigated for ^{6}He projectile on different target charges and beam energies. It is concluded that close to the Coulomb barrier, coupling to Coulomb dipole breakup should be evident only in scattering with targets having high charge ($Z_T \approx 80$) and that measurements with lighter targets ($Z_T \approx 28$) are not sensitive to this coupling. ^{11}Be has strong low-lying continuum dipole strength, as ^{6}He. The observation of a strong reduction of the Coulomb-nuclear interference peak (CNIP) in the scattering of ^{11}Be with a light charge target must be due to other mechanisms besides coupling to Coulomb breakup. These mechanisms could be associated with the halo structure. In ^{6}He-induced collisions, a clear reduction of the elastic scattering in the CNIP region is observed, although not as large as in the present case only for heavy targets [22]. The ^{6}He elastic-

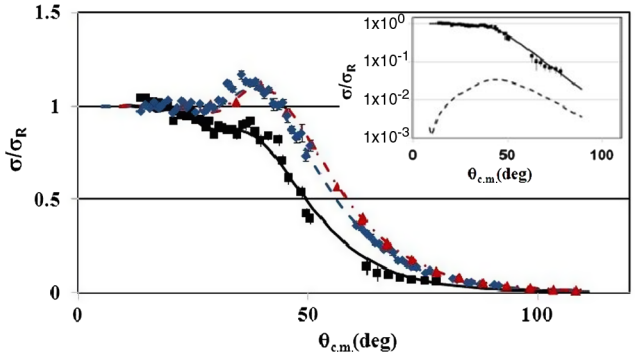

FIG. 1 (color online). Elastic-scattering angular distributions on ^{64}Zn: ^{9}Be (triangles), ^{10}Be (diamonds), and ^{11}Be (squares). The lines represent the OM calculations for ^{9}Be (dot-dashed line), ^{10}Be (dashed line), and ^{11}Be (full line). The inset shows the measured AD (symbols) and OM fit (full line) for the ^{11}Be + ^{64}Zn system together with the result of the calculation for the inelastic excitation of ($\frac{1}{2}^{-}$, $E_x = 0.32$ MeV, dashed line). The error bars are statistical for ^{10,11}Be and statistical + systematic for ^{9}Be on ^{64}Zn. See text for details.

scattering AD on the same medium mass ^{64}Zn target does not show such a feature [13]. The observed difference in ^{6}He and ^{11}Be scattering could be due to the more extended halo distribution in ^{11}Be compared to ^{6}He (e.g., [23]).

In the experiment with the ^{11}Be beam an unusual large yield of direct transfer or breakup processes is observed. In Fig. 2 we compare ΔE-E spectra for collisions induced by ^{10}Be and ^{11}Be. The collision induced by ^{11}Be shows events close to the elastic, consistent with the detection of ^{10}Be coming from transfer and/or breakup processes; such events are not observed with the ^{10}Be beam. In Fig. 3 the AD for such events is shown; the corresponding integrated cross section, obtained by assuming $\frac{d\sigma}{d\theta} = 0$ at $\theta_{\rm lab} = 0$ and 60°, is $\sigma = 1100 \pm 150$ mb.

The ^{9,10,11}Be + ^{64}Zn elastic-scattering data were analyzed within the optical model (OM) using the code PTOLEMY [24]. For ^{9,10}Be a Woods-Saxon (WS) form of the real and imaginary potential was used. To avoid a fit with too many free parameters, the radius and diffuseness (real and imaginary) were fixed. Before fixing these parameters, their effect was evaluated by performing fits with different values, varying them at steps of 0.05 fm. Having fixed the geometry of the WS potential, the best χ^2 was searched by varying the potential depths, and the results are shown in Fig. 1. In the case of ^{11}Be, in order to have a better fit, a surface term was added to the imaginary volume potential.

It is known that when bombarding energies approach the top of the Coulomb barrier, coupling effects become important. They are responsible for the ''threshold anomaly,'' i.e., the rapid variation with energy of the optical potentials (OP) needed to reproduce elastic-scattering data. Couplings can be represented in the OM by the addition of a complex dynamic polarization potential (DPP) to the OP (see, e.g., [25] and references therein). In [26] the DPP was a surface potential calculated analytically and applied to the ^{11}Be + ^{12}C data at 49.3 AMeV. The real part of the DPP was not considered in the calculations since it produced a negligible effect on the elastic-scattering fit. The volume potential, responsible for the inelastic core-target interaction, was obtained from the fit of the scattering of the ^{10}Be core on the same target. The calculated surface potential was responsible for peripheral reactions such as transfer or breakup. This term has an exponential tail, and a diffuseness parameter of 3.2 fm. A similar result was also obtained in [23]. This diffuseness depends on the projectile characteristics and not on the target; it is in fact related to the decay length of the neutron initial state wave function [26]. We used a procedure similar to [26] to deduce the OP in the case of ^{11}Be + ^{64}Zn. In the present case, all terms of the OP were extracted phenomenologically from a fit of the elastic-scattering AD. We performed the fit of ^{11}Be + ^{64}Zn using, as the volume part of the real and imaginary WS potentials, the ones obtained from the fit of the elastic scattering of the core ^{10}Be on ^{64}Zn. In addition, we considered a surface term having the shape of a WS derivative. The fit of ^{11}Be + ^{64}Zn scattering was performed having as free parameter the surface potential depth and varying the surface diffuseness at steps of 0.05 fm. The best χ^2 are obtained for a_{si} around 3.5 fm. Equivalent good fits, obtained by varying a_{si} around this value, give the same σ_R within 4%. Both surface diffuseness and potential depth extracted from the fit are consistent with [26]. The potential parameters are shown in Table I. As mentioned above, the large diffuseness is related to the decay length of the neutron initial state wave function and is necessary in order to reproduce the behavior of the elastic cross section at the CNIP. The suppression of the cross section at the CNIP is originated by absorption occurring at large partial waves due to diffuse halo structure of ^{11}Be. In Fig. 4, the module of the reflection coefficients is shown as a function of l for

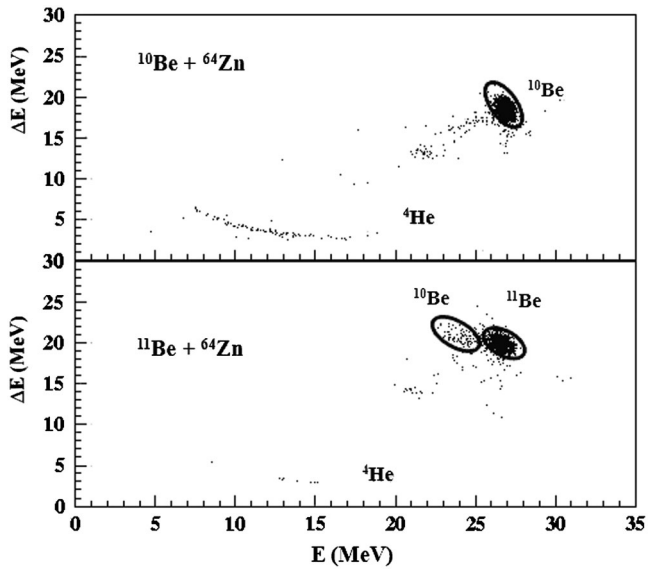

FIG. 2. ΔE-E scatter plots for the reactions ^{10}Be + ^{64}Zn (top) and ^{11}Be + ^{64}Zn (bottom), at $\theta = 35°$.

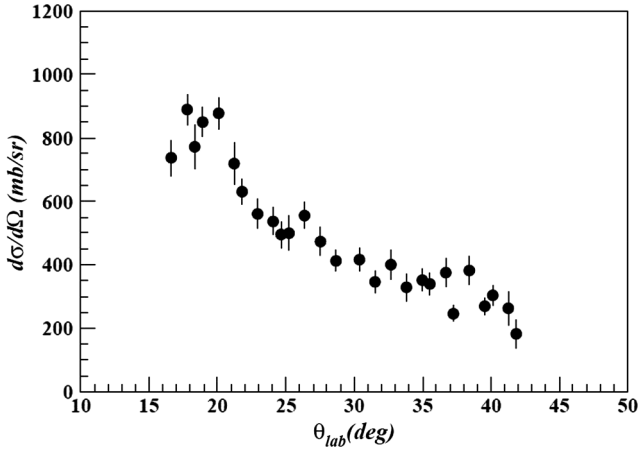

FIG. 3. AD of transfer or breakup events in ^{11}Be + ^{64}Zn obtained by selecting ^{10}Be events in the ΔE-E spectrum.

TABLE I. WS optical potentials obtained from the fit of the experimental data. The real potential radius parameter is $r_0 = 1.1$ fm and the imaginary one is $r_i = 1.2$ fm, where $R_{0,i,si} = r_{0,i,si}(A_p^{1/3} + A_t^{1/3})$. The Coulomb radius parameter is $r_C = 1.25$ fm.

Reaction	V (MeV)	a (fm)	V_i (MeV)	a_i (fm)	V_{si} (MeV)	r_{si} (fm)	a_{si} (fm)	J_V (MeV fm^3)	J_W (MeV fm^3)
^{9}Be + ^{64}Zn	126	0.6	17.3	0.75				295	53
^{10}Be + ^{64}Zn	86.2	0.7	43.4	0.7				193	124
^{11}Be + ^{64}Zn	86.2	0.7	43.4	0.7	0.151	1.3	3.5	193	129

the three reactions ^{9,10,11}Be + ^{64}Zn, as obtained from the OM fit. The behavior at large l in the ^{11}Be-induced collision clearly reflects the long range of the absorptive surface potential. According to [2] the effect of long-range absorption is twofold: (1) it damps the Coulomb amplitude at angles lower than the ''grazing'' and (2) smooths out the trend of $|S(l)|$ at the nuclear surface. Both these features are observed in the present ^{11}Be + ^{64}Zn data.

The possible contribution to the scattering cross section of the 1st excited state of ^{11}Be, which we were not able to separate from the elastic, was evaluated by calculating the Coulomb excitation cross section with the dipole strength $B(E1) = 0.115e^2$ fm^2 [27]. It is noted that the nuclear contribution is estimated to be less than 1%. These calculations show that the inelastic contribution to the scattering cross section is very small. This can be seen in the inset of Fig. 1. The TR cross sections deduced from OM analysis are $\sigma_R = 1090$ mb for ^{9}Be, $\sigma_R = 1260$ mb for ^{10}Be, and $\sigma_R = 2730$ mb for ^{11}Be. A much larger TR cross section is therefore measured in the halo nucleus case. The transfer or breakup cross section extracted from Fig. 3 corresponds to about 40% of the TR cross section. This result confirms what was found in the ^{6}He experiments (e.g., [13,14]) but disagrees with the results of [17]. The reason for that could be the inclusion of breakup or transfer events in the ^{11}Be + ^{209}Bi quasielastic data due to the poor beam energy resolution and the lack of particle identification.

In summary, the collisions ^{9,10,11}Be + ^{64}Zn have been measured at a center of mass energy of ≈ 24.5 MeV. While the shape of the elastic-scattering AD is the same for ^{9}Be and ^{10}Be isotopes, the scattering of the ^{11}Be halo nucleus shows extremely different features. The peak due to Coulomb-nuclear interference disappears and absorption occurs at much smaller scattering angles (i.e., much larger impact parameters) than for the other two Be isotopes. The data were interpreted within the OM. In order to reproduce the ^{11}Be data, we added to the volume core-target OM potential (extracted from the ^{10}Be + ^{64}Zn data) a surface potential to take into account the diffuse halo structure. The best fits were obtained with a surface term having a very large diffuseness, in agreement with what was found in [26]. From the OM analysis, the TR cross sections were also extracted. In the halo nucleus case this cross section is about a factor of 2 larger than for the ^{9,10}Be + ^{64}Zn reactions. From the observation of ^{10}Be ejectiles in ^{11}Be-induced collisions, it was found that about 40% of the TR cross section can be attributed to transfer and/or breakup. These results show, for the first time, a strong effect on nuclear reaction mechanisms around the Coulomb barrier due to the ^{11}Be halo structure. This represents an independent confirmation that similar effects observed for ^{6}He are also due to its halo nature.

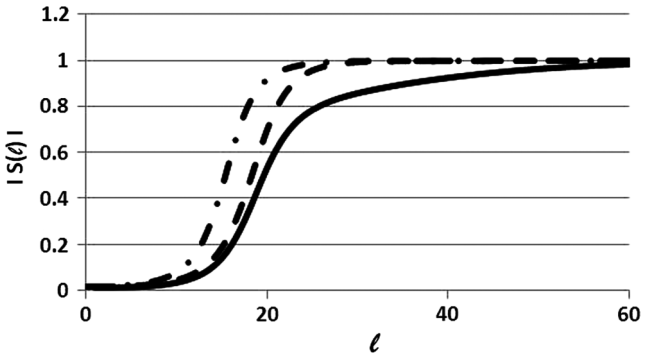

FIG. 4. The absolute $S(l)$ distribution for ^{9}Be + ^{64}Zn (dot-dashed line), ^{10}Be + ^{64}Zn (dashed line), and ^{11}Be + ^{64}Zn (full line) extracted from the OM fit.

We wish to thank Dr. A. Bonaccorso for reading and commenting on the manuscript. This work has been supported by INFN, by the European Commission Sixth Framework Program—EURONS (Contract No. 506065), and by Contract No. FPA2007-63074 of Spanish Ministery of Science.

*Present address: LPC-ENSICAEN, IN2P3-CNRS and Université de Caen, Caen, France.
†Present address: Departamento de Fisica Atomica, Molecular y Nuclear, Universidad Complutense, Madrid, Spain.
‡Present address: Nuclear Science Division, Lawrence Berkeley National Laboratory, Berkeley, CA, USA.

[1] E. Rutherford, Philos. Mag. **21**, 669 (1911).
[2] S. Fricke *et al.*, Nucl. Phys. **A500**, 399 (1989).
[3] A. Jensen *et al.*, Rev. Mod. Phys. **76**, 215 (2004).
[4] Y. Kucuk *et al.*, Phys. Rev. C **79**, 067601 (2009).
[5] A. M. Moro *et al.*, Phys. Rev. C **75**, 064607 (2007).
[6] T. Matsumoto *et al.*, Phys. Rev. C **73**, 051602(R) (2006).
[7] M. Rodríguez-Gallardo *et al.*, Phys. Rev. C **77**, 064609 (2008).
[8] K. Rusek *et al.*, Phys. Rev. C **72**, 037603 (2005).
[9] N. Keeley and N. Alamanos, Phys. Rev. C **77**, 054602 (2008).

[10] A. Chatterjee *et al.*, Phys. Rev. Lett. **101**, 032701 (2008).
[11] N. Keeley *et al.*, Prog. Part. Nucl. Phys. **63**, 396 (2009).
[12] N. Keeley *et al.*, Prog. Part. Nucl. Phys. **59**, 579 (2007).
[13] A. Di Pietro *et al.*, Phys. Rev. C **69**, 044613 (2004).
[14] E. Aguilera *et al.*, Phys. Rev. C **63**, 061603(R) (2001).
[15] P. D. Young *et al.*, Phys. Rev. C **71**, 051601 (2005).
[16] M. Mazzocco *et al.*, Eur. Phys. J. A **28**, 295 (2006).
[17] M. Mazzocco *et al.*, Eur. Phys. J. Special Topics **150**, 37 (2007).
[18] L. Acosta *et al.*, Eur. Phys. J. A **42**, 461 (2009).
[19] M. Freer, Rep. Prog. Phys. **70**, 2149 (2007).
[20] I. Tanihata *et al.*, Phys. Lett. B **206**, 592 (1988).
[21] W. Love *et al.*, Nucl. Phys. **A291**, 183 (1977).
[22] A. M. Sánchez-Benítez *et al.*, Nucl. Phys. **A803**, 30 (2008).
[23] M. Hassan *et al.*, Phys. Rev. C **79**, 064608 (2009).
[24] M. Rhoades-Brown *et al.*, Phys. Rev. C **21**, 2417 (1980).
[25] G. Satchler, Phys. Rep. **199**, 147 (1991).
[26] A. Bonaccorso and F. Carstoiu, Nucl. Phys. **A706**, 322 (2002).
[27] F. Ajzenberg-Selove, Nucl. Phys. **A506**, 1 (1990).